

Conduction anisotropy and Hall effect in the organic conductor $(\text{TMTTF})_2\text{AsF}_6$: evidence for Luttinger liquid and charge ordering

Bojana Korin-Hamzić*

Institute of Physics, P.O.Box 304, HR-10001 Zagreb, Croatia

Emil Tafra, Mario Basletić and Amir Hamzić

Department of Physics, Faculty of Science, P.O.Box 331, HR-10002 Zagreb, Croatia

Martin Dressel

1. Physikalisches Institut, Universität Stuttgart, Pfaffenwaldring 57, D-70550 Stuttgart, Germany

(Dated: November 13, 2018)

We present the high-temperature ($70\text{ K} < T < 300\text{ K}$) resistivity anisotropy and Hall effect measurements of the quasi-one-dimensional (1D) organic conductor $(\text{TMTTF})_2\text{AsF}_6$. The temperature variations of the resistivity are pronouncedly different for the three different directions, with metallic-like at high temperatures for the **a**-axis only. Above 220 K the Hall coefficient R_H is constant, positive and strongly enhanced over the expected value; and the corresponding carrier concentration is almost 100 times lower than calculated for one hole/unit cell. Our results give evidence for the existence of a high-temperature regime above 200 K where the 1D Luttinger liquid features appear in the transport properties. Our measurements also give strong evidence of charge ordering in $(\text{TMTTF})_2\text{AsF}_6$. At the charge-ordering transition $T_{\text{CO}} \approx 100\text{ K}$, $R_H(T)$ abruptly changes its behavior, switches sign and rapidly increases with further temperature decrease.

PACS numbers: 71.20.Rv, 71.27.+a, 71.30.+h, 72.15.Gd, 71.10.Pm

I. INTRODUCTION

The highly anisotropic organic conductors with their very rich phase diagram turn out to be excellent choice for exploring the phenomena of one-dimensional physics.¹ It is well established theoretically that the conventional Fermi-liquid (FL) theory of 3D metals does not apply to interacting electrons when the motion is confined to one dimension. Instead, the Luttinger liquid (LL) approach is valid, where the quasi-particle FL excitations are replaced by separate collective spin and charge excitations, propagating with different velocities.^{2,3} LL systems exhibit non-FL like power-law behavior in temperature and energy, and the exponents are interaction-dependent. When coupling between the chains is relevant, a crossover from the LL to a coherent (FL) behavior is expected as the temperature (or frequency) is lowered.⁴

The quasi-1D character of the electronic structure of $(\text{TMTCF})_2X$ ($C = \text{Se}$, tetramethyltetraselenafulvalene; $C = \text{S}$, tetramethyltetrathiofulvalene; anion $X^- = \text{PF}_6^-$, AsF_6^- , ReO_4^- , ...) materials is a consequence of their crystallographic structure. The large planar TMTCF molecules form segregated molecular columns (chains) where the molecular orbitals overlap along the columns, giving rise to the highest conductivity direction (**a**). The separation of the columns limits the coupling in the perpendicular directions. The anisotropy of the tight-binding overlap integrals along the three directions is $t_a : t_b : t_c \approx 1 : 0.1 : 0.005$ for the high (**a**), intermediate (**b**) and weak (**c**) coupling/conductivity directions respectively.¹ Charge transfer of one electron from the chains to each of the anions results in quarter-filled hole bands on the TMTCF stacks (or half-filled, if the dimer-

ization along the chain is taken into account). It is also well known that exchanging Se for S and/or using a different anion X leads to the unified phase diagram for the $(\text{TMTCF})_2X$ series that spans from more anisotropic $C = \text{S}$ to $C = \text{Se}$, where the properties of one compound at a given pressure are analogous to those of another compound under higher pressure.⁵

Selenium based $(\text{TMTSF})_2X$ salts exhibit a high conductivity at room temperature and a metallic behavior down to low temperatures, where the incommensurate spin-density-wave (SDW) ground state is established. Like other $C = \text{S}$ salts that are more anisotropic, i.e. more 1D, $(\text{TMTTF})_2\text{AsF}_6$ is typically 20 (or more) times less conducting than $C = \text{Se}$ salts at room temperature.^{6,7} Below a broad minimum near $T_\rho \approx 240\text{ K}$ (attributed to the opening of a charge gap Δ_ρ and considered to be a continuous charge localization due to the anion potential – lattice dimerization), the resistivity of $(\text{TMTTF})_2\text{AsF}_6$ increases on cooling and the system becomes a very good insulator at low temperatures ($T < 20\text{ K}$), where the spin-Peierls transition occurs. The spin susceptibility remains unaffected by the charge localization despite the thermal activation of carriers below T_ρ , indicating the decoupling between the spin and charge degrees of freedom. The anomaly in resistivity at $T_{\text{CO}} \approx 100\text{ K}$ has been recently clarified by the discoveries of the huge anomaly in the dielectric constant ϵ (Ref. 8) and of the charge ordering (CO) seen by nuclear magnetic resonance (NMR), electron spin resonance (ESR) and optical experiments.^{9,10,11,12} The nature of this phase transition was interpreted as a ferroelectric (FE) state, which is supported by the clear-cut fit of the anomaly in $\epsilon(T)$ to a Curie law. The FE transition is followed by

a steep increase of the conductivity gap Δ but with no appearance of a spin gap.

There is still no general agreement whether the transport properties of quasi-1D (TMTCF)₂X salts at high temperatures ($T > 200$ K) – where the thermal energy exceeds the transverse coupling and the coherence for the interchain transport is lost – should be understood in terms of usual FL theory or LL theory.^{7,13} For example, there are indications of spin-charge separation by the similarity in the spin dynamics and thermal conductivity for $C = S$ and $C = Se$ salts, but the electronic transport is very different.

Further, the absence of a plasma edge for polarization perpendicular to the chains in (TMTTF)₂X salts suggests that the electrons are confined on the chains, which is not the case for (TMTSF)₂X compounds. However, while the dc conductivities along the chain axis \mathbf{a} in the latter compounds are metallic-like, the finite frequency response is not that of a simple Drude metal and the optical conductivity data for (TMTCF)₂X salts were interpreted as a strong evidence for non-FL behavior: the power law asymptotic dependence of the high frequency optical mode has been addressed to LL exponents.¹⁴ It was concluded that all the dc transport is due to a very narrow Drude peak, containing only 1% of the spectral weight, whereas the remaining 99% is above an energy gap (of the order of 200 cm^{-1}) and reminiscent of a Mott insulating structure. These results agree with the LL theoretical predictions based on the doped Hubbard chains, yielding a gap feature and a zero-frequency mode with a small spectral weight (this mode is responsible for the metallic conductivity).¹⁵ One would expect that such a reduction of the carrier concentration n (participating in the dc transport) should manifest itself in an enhanced value of the Hall coefficient. However, so far the high temperature Hall effect measurements were performed for (TMTSF)₂X compounds only, and did not confirm these expectations; moreover, the results for (TMTSF)₂PF₆ were interpreted differently, i.e. using the conventional FL theory¹⁶ and LL concept.¹⁷ Recently, we have investigated the metallic state of (TMTSF)₂ReO₄ (more anisotropic than the $X = \text{PF}_6$), aiming to shed more light on FL or LL concepts from transport measurements and particularly Hall effect.¹⁸ The pronounced conductivity anisotropy, a small and smoothly temperature dependent Hall effect (where the obtained R_H values indicate that all the carriers contribute to the metallic-like transport) and a small, positive and temperature dependent magnetoresistance were analyzed within FL and non-FL models: although not fully conclusive, these data nevertheless favor the FL description. We have also proposed that the possible appearance of the LL features in the transport properties should be found in the more anisotropic (TMTTF)₂X series, where the interchain interactions play a minor role. The present study of the temperature dependence of the resistivity anisotropy and the Hall effect in (TMTTF)₂AsF₆ is therefore a step forward in the identification of the LL features in the trans-

port properties of $C = S$ compounds. In addition, our study gives strong evidence for a charge ordering transition from transport properties.

II. EXPERIMENT

The measurements were conducted in the high temperature region $70 \text{ K} < T < 300 \text{ K}$. The single crystals came all from the same batch and exhibit the same behavior. The resistivity data, that will be analyzed here, are for \mathbf{a} , \mathbf{b}' and \mathbf{c}^* axis. The \mathbf{a} direction is the highest conductivity direction, the \mathbf{b}' direction (with intermediate conductivity) is perpendicular to \mathbf{a} in the \mathbf{a} - \mathbf{b} plane and the \mathbf{c}^* direction (with the lowest conductivity) is perpendicular to the \mathbf{a} - \mathbf{b} (and \mathbf{a} - \mathbf{b}') plane. For \mathbf{b}' and \mathbf{c}^* -axis resistivity measurements, the samples have been cut from a long crystal along \mathbf{a} axis, and the contacts were placed on the opposite \mathbf{a} - \mathbf{c}^* ($\rho_{\mathbf{b}'}$) and \mathbf{a} - \mathbf{b}' ($\rho_{\mathbf{c}^*}$) surfaces with gold wires stuck by silver paint. The samples were cooled slowly (3 K/hour) in order to avoid irreversible resistance jumps (caused by micro-cracks), well known to appear in all organic conductors.

The Hall effect was measured in standard geometry ($\mathbf{j} \parallel \mathbf{a}$, $\mathbf{B} \parallel \mathbf{c}^*$) for temperatures $70 \text{ K} < T < 300 \text{ K}$ and in magnetic field up to 9 T. Two pairs of Hall contacts and one pair of current contacts were made on the sides of the crystal by evaporating gold pads and attaching $30 \mu\text{m}$ diameter gold wires with silver paint.¹⁹ AC current (10 μA to 1 mA, 22 Hz) was applied. DC technique was used at lower temperatures, because of the large resistance increment. Particular care was taken to ensure the temperature stabilization. The Hall voltage was measured at fixed temperatures for both pairs of Hall contacts to test and/or control the homogenous current distribution through the sample and in field sweeps from $-B_{\text{max}}$ to $+B_{\text{max}}$ in order to eliminate the possible mixing of magnetoresistive components. The Hall coefficient R_H was obtained as $R_H = (V_{xy}/IB)t$, where V_{xy} is Hall voltage determined as $[V_{xy}(B) - V_{xy}(-B)]/2$, I is the current through the crystal and t is the sample thickness.

III. RESULTS

Figure 1 shows the temperature dependence of the resistivity, $\rho(T)$ vs. $1/T$, for (TMTTF)₂AsF₆ in the temperature range $70 \text{ K} < T < 300 \text{ K}$, measured along the three crystal directions. The room temperature conductivity values for $\sigma_{\mathbf{a}}$ ($\mathbf{j} \parallel \mathbf{a}$), $\sigma_{\mathbf{b}'}$ ($\mathbf{j} \parallel \mathbf{b}'$) and $\sigma_{\mathbf{c}^*}$ ($\mathbf{j} \parallel \mathbf{c}^*$) are $(15 \pm 5) (\Omega\text{cm})^{-1}$, $(0.3 \pm 0.1) (\Omega\text{cm})^{-1}$ and $(1.5 \pm 0.5) \times 10^{-3} (\Omega\text{cm})^{-1}$, respectively. The $\rho_{\mathbf{a}}(T)$ results are in good agreement with the previously published data,^{6,20} while $\rho_{\mathbf{b}'}(T)$ and $\rho_{\mathbf{c}^*}(T)$ were not measured up to now. The resistivity (ρ vs. T) data above 230 K are shown in more details in Fig. 2. One can observe the pronounced difference in temperature dependencies of resistivities for three different directions. The metallic-like behavior is

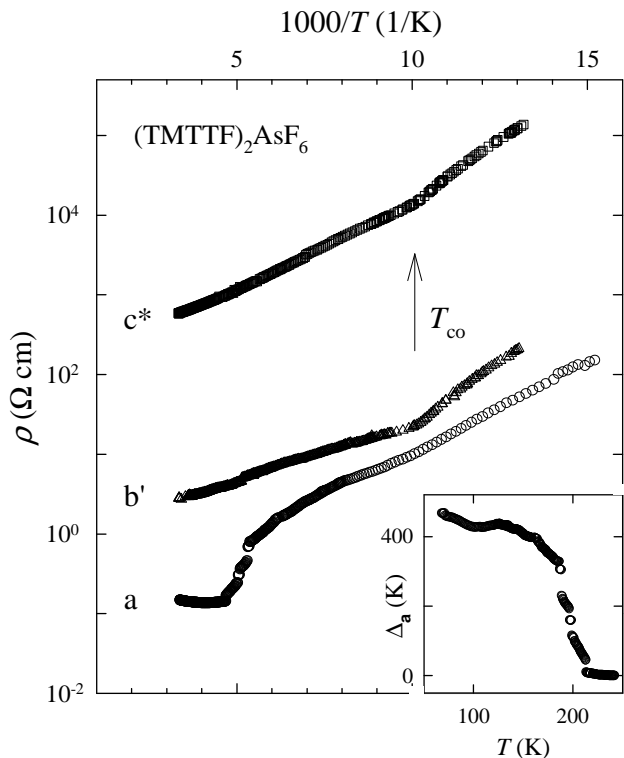


FIG. 1: Temperature dependence of the dc resistivity, ρ vs. $1/T$, for $(\text{TMTTF})_2\text{AsF}_6$ in the temperature range $70 \text{ K} < T < 300 \text{ K}$, measured along the three crystal directions: $\rho_{\mathbf{a}}$ ($\mathbf{j} \parallel \mathbf{a}$), $\rho_{\mathbf{b}'}$ ($\mathbf{j} \parallel \mathbf{b}'$) and $\rho_{\mathbf{c}^*}$ ($\mathbf{j} \parallel \mathbf{c}^*$). Inset: Activation energy $\Delta_{\mathbf{a}}$ vs. temperature calculated for the \mathbf{a} -axis assuming $\Delta_{\mathbf{a}} = k_B T \ln(\rho_{\mathbf{a}}/\rho_{\min})$ - see text.

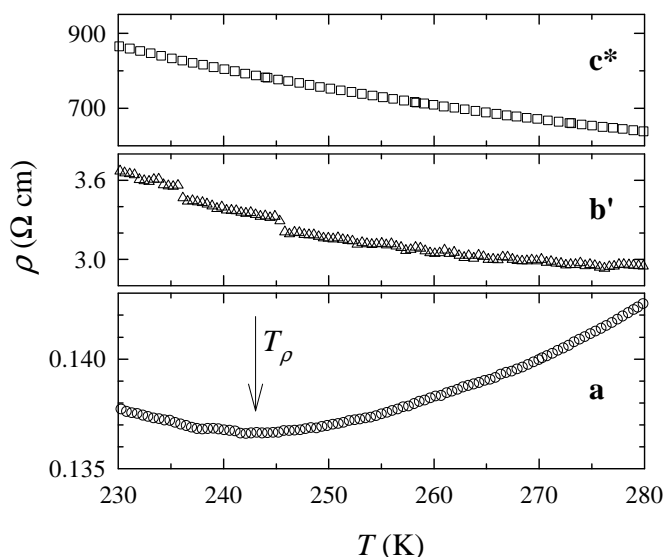


FIG. 2: Temperature dependencies of the resistivity along the \mathbf{a} , \mathbf{b}' and \mathbf{c}^* axes for $(\text{TMTTF})_2\text{AsF}_6$ in the high-temperature region ($T > 230 \text{ K}$).

found only for the highest conductivity direction \mathbf{a} , above 240 K , and it can be described by a $\rho_{\mathbf{a}} \propto T^{0.75}$ law. Below a broad minimum around $T_{\rho} \approx 240 \text{ K}$, the resistivity $\rho_{\mathbf{a}}$ increases on cooling and this is attributed to the continuous opening of a charge gap: below 240 K , $\rho_{\mathbf{a}}(T)$ can be analyzed using a phenomenological law for a semiconductor $\rho_{\mathbf{a}}(T) = \rho_{\min} \exp[\Delta_{\mathbf{a}}/k_B T]$. In this expression all the thermal evolution of the resistivity $\rho_{\mathbf{a}}(T)$ is included in the function $\Delta_{\mathbf{a}}(T)$, defined as a temperature-dependent energy gap, while the prefactor ρ_{\min} is determined as $\rho(T_{\rho})$ i.e. the resistivity value just above $T_{\rho} \approx 240 \text{ K}$. $\Delta_{\mathbf{a}}(T)$ is zero at T_{ρ} and its value gradually rises to almost 400 K down to T_{CO} . At the charge-ordering transition T_{CO} there is the change in slope, and a step increase of the conductivity gap Δ is observed, yielding $\Delta_{\mathbf{a}}(T < T_{\text{CO}}) \approx 480 \text{ K}$ (see inset of Fig. 1). T_{CO} is explained as the temperature where a spontaneous charge disproportionation, called charge ordering (CO), occurs.

On the other hand, there are no indications of a metallic-like behavior along neither of the two perpendicular directions (along \mathbf{b}' or \mathbf{c}^* axis). Below room temperature and in the temperature region where $\rho_{\mathbf{a}}(T)$ is metallic-like, for both \mathbf{b}' and \mathbf{c}^* axis we have found that the resistivity increase with decreasing temperature (Fig. 2). These data could be fitted to $\rho_{\mathbf{b}'}(T) \propto T^{-0.5}$ and $\rho_{\mathbf{c}^*}(T) \propto T^{-1.27}$ at high temperatures. Note also that there is no change in slope for neither $\rho_{\mathbf{b}'}(T)$ nor $\rho_{\mathbf{c}^*}(T)$ around T_{ρ} , i.e. at the temperature where the resistivity minimum is observed for the \mathbf{a} direction. Instead, for the \mathbf{b}' and \mathbf{c}^* axes the resistivity increases exponentially down to $T_{\text{CO}} \approx 100 \text{ K}$, and the respective conductivity gaps achieve similar values as for the \mathbf{a} axis: $\Delta_{\mathbf{b}'} = (350 \pm 50) \text{ K}$ and $\Delta_{\mathbf{c}^*} = (400 \pm 50) \text{ K}$. Below T_{CO} there is a sharper change of slope than for \mathbf{a} axis, indicating an increased conductivity gap value $\Delta_{\mathbf{b}'}(T < T_{\text{CO}}) \approx \Delta_{\mathbf{c}^*}(T < T_{\text{CO}}) \approx 600 \text{ K}$.

To our knowledge, no Hall experiments have been performed in any representative of the $(\text{TMTTF})_2X$ -family up to now. The magnetic field dependence of the Hall resistivity of $(\text{TMTTF})_2\text{AsF}_6$ is shown in Fig. 3 for three representative temperatures. These data confirm that the Hall resistivity is linear with field up to 9 T in the whole temperature interval we have investigated.

Figure 4 shows the temperature dependence of the Hall coefficient R_H of $(\text{TMTTF})_2\text{AsF}_6$ for $70 \text{ K} < T < 300 \text{ K}$. (We note here that the results for another crystal from the same batch showed similar behavior). The inset of Fig. 4 shows (in more details) the same results around the maximum in R_H . The Hall coefficient is positive from room temperature down to about 95 K where it changes sign; then its (negative) value rapidly increases with further temperature decrease. Note that the change in sign occurs around T_{CO} , i.e. at the temperature where an increase of the conductivity gap Δ is found in resistivity measurements.

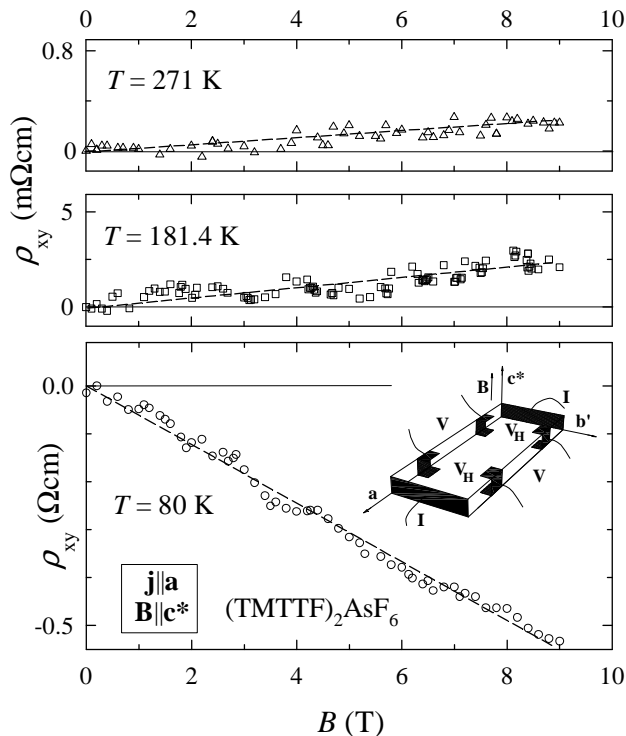


FIG. 3: Magnetic field dependence of the Hall resistivity of $(\text{TMTTF})_2\text{AsF}_6$ for several fixed temperatures. Also shown is the sample geometry ($\mathbf{j} \parallel \mathbf{a}$, $\mathbf{B} \parallel \mathbf{c}^*$) and the arrangement of contacts.

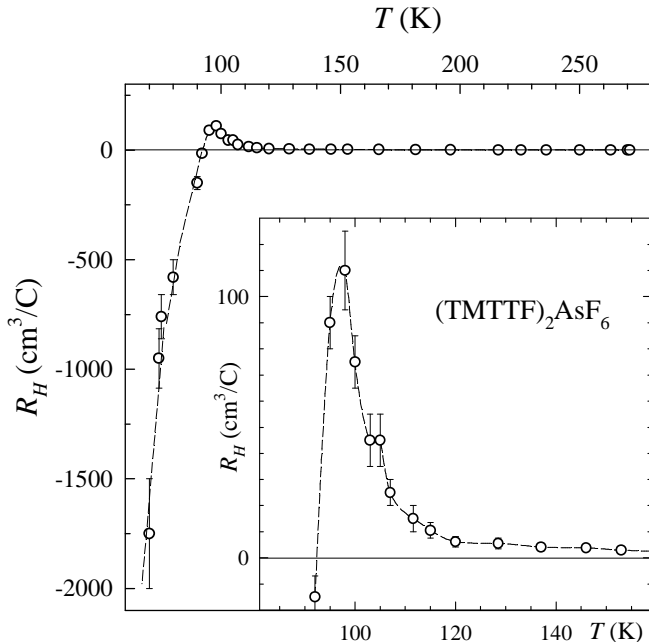


FIG. 4: Temperature dependence of the Hall coefficient R_H of $(\text{TMTTF})_2\text{AsF}_6$ for $70 \text{ K} < T < 300 \text{ K}$. For each temperature the Hall coefficient values were determined as the average of the several measurements taken during the cooling and heating cycles. Inset: $R_H(T)$ around T_{CO} .

IV. DISCUSSION

A. Resistivity

Let us start by pointing out that it is for the first time that in a member of the $(\text{TMTCF})_2X$ -salt family a metallic-like temperature variation of the resistivity at high temperatures has been found for \mathbf{a} axis only. Although only poorly investigated up to now, for the Se-compounds the \mathbf{b}' -axis resistivity seems to follow also a metallic-like decrease upon lowering the temperature, while for \mathbf{c}^* axis the results varied – from metallic to semiconducting-like, depending on X .^{18,21,22,23} On the other hand, as far as we know, there are no published data on detailed resistivity anisotropy measurements for the sulphur analogs $(\text{TMTTF})_2X$.

The simplest model of the FL electron transport in metals is the Drude theory, where all the relaxation processes are described by a single relaxation time τ .²⁴ In first approximation, lattice and electronic interactions only renormalize the relevant quantities, leading to some effective carrier mass, for instance. No matter how strong the anisotropy of the parameters is, the underlying transport mechanisms should be similar in all three directions leading to a similar dependence on temperature. Consequently, this model cannot describe the obvious differences in the temperature dependences of $\rho_{\mathbf{a}}$, $\rho_{\mathbf{b}'}$ and $\rho_{\mathbf{c}^*}$, and therefore the resistivity measurements provide evidence against a conventional FL picture. In particular, the fact that the metallic-like behavior is found at high temperature for $\rho_{\mathbf{a}}$ only (for $T > 240 \text{ K}$), further supports this opinion.

Within the model of a Luttinger liquid the transport properties were also calculated for a system of weakly coupled chains, resulting in quantities like the in-plane conductivity (σ_{\parallel}), inter-plane conductivity (σ_{\perp}) and Hall effect.^{25,26} It was found that the inter-chain hopping is responsible for the metallic character of the $(\text{TMTCF})_2X$ compounds, which otherwise would be Mott insulators. Namely, the interchain hopping can be viewed as an effective doping, leading to deviations from the commensurate filling, which would be insulating. For longitudinal (ρ_{\parallel}) and transverse (ρ_{\perp}) resistivity, the temperature power law was calculated, giving $\rho_{\parallel}(T) \propto T^{16K_{\rho}-3}$ and $\rho_{\perp}(T) \propto T^{1-2\alpha}$. K_{ρ} is the LL exponent controlling the decay of all correlation functions ($K_{\rho} = 1$ corresponds to non-interacting electrons and $K_{\rho} < 0.25$ is the condition upon which the $1/4$ filled umklapp process becomes relevant) and $\alpha = (K_{\rho} + 1/K_{\rho})/4 - 1/2$ is the Fermi surface exponent.⁴

The large pressure coefficient of the conductivity in the metallic regime for $(\text{TMTCF})_2X$ salts ($\delta \ln \sigma / \delta P$ up to $25\% \text{ kbar}^{-1}$ around room temperature) raises a problem for the comparison of experimental data with theory, which usually computes constant-volume temperature dependencies.²⁷ Namely, it is known that in most organic conductors much of the temperature dependence

of the conductivity, at high temperatures, arises from the thermal expansion. As a consequence, the constant pressure data show usually different temperature dependencies than constant-volume data. Note that all the data presented in Fig. 1 are measured at ambient pressure and usually considered as the constant-pressure data. Therefore, the conversion from the constant-pressure $\rho(T)$ data in Fig. 1 to the constant-volume $\rho^{(V)}(T)$ data has to be performed, in order to compare the experimental results with theoretical models. This conversion procedure was performed for $(\text{TMTSF})_2\text{PF}_6$, where the unit cell, at 4.2 K and at ambient pressure, was taken as the reference unit cell.⁵ Here, the thermal expansion, the compressibility data and transport data under various pressures would have to be taken into account. Since we do not know these data for $(\text{TMTTF})_2X$ compounds, we have followed the same procedure as it was performed for $(\text{TMTSF})_2X$ isostructural compounds. However, $(\text{TMTTF})_2X$ salts have an approximately 5% smaller unit-cell volume, about 2% smaller lattice parameters and about 30% higher t_{\parallel}/t_{\perp} ratio at 300 K (calculated using the tight-binding scheme^{1,28}) than $(\text{TMTSF})_2X$ salts, and therefore the conversion procedure has to be taken with some precaution. We have used the expression $\rho_{\mathbf{a},\mathbf{b}'}^{(V)} = \rho_{\mathbf{a},\mathbf{b}'} / [1 + (\delta \ln \sigma / \delta P)P]$, where P is the pressure that must be applied at given T in order to restore the reference volume. We have exploited the P values from Ref. 5 and used in Ref. 18, and we have taken $\delta \ln \sigma / \delta P = 0.10$ (i.e. the same value as in Ref. 23). For $\rho_{\mathbf{c}^*}^{(V)}$ the corrections were not made because the data for \mathbf{c}^* axis resistivity in $(\text{TMTSF})_2\text{PF}_6$ were calculated differently and P values are not available.²⁹

In the case of the \mathbf{a} -axis resistivity of $(\text{TMTSF})_2\text{PF}_6$, the conversion from experimentally obtained constant-pressure behavior $\rho_{\mathbf{a}}(T) \propto T^{1.8}$ yielded an almost linear constant-volume dependence $\rho_{\mathbf{a}}^{(V)}(T) \propto T^{0.85}$ (Ref. 5). Nearly linear $\rho_{\mathbf{a}}$ vs. T is expected within existing FL and LL theoretical models (in this case for $K_{\rho} \approx 0.23$ obtained from optical measurements).^{25,30} Our experimental \mathbf{a} -axis resistivity results for $(\text{TMTTF})_2\text{AsF}_6$ show that already under constant-pressure condition we obtain a smoother temperature dependence $\rho_{\mathbf{a}}(T) \propto T^{0.75}$ (for $T > 260$ K), i.e. even without conversion it is rather close to a linear temperature dependence (the corresponding K_{ρ} has about the same values as for $(\text{TMTSF})_2\text{PF}_6$). Nevertheless, the conversion procedure has to be performed and this yields the constant-volume temperature dependencies $\rho_{\mathbf{a}}^{(V)}(T) \propto T^{0.22}$ and $\rho_{\mathbf{b}'}^{(V)}(T) \propto T^{-0.6}$ (as shown in Fig. 5). From the obtained exponent values we found $K_{\rho} = 0.20$ and $\alpha = 0.8$. Our K_{ρ} is lower than 0.23 calculated for $(\text{TMTSF})_2X$ compounds: although this difference could be the consequence of a crude approximation in the conversion procedure, it is worth noting that a somewhat lower K_{ρ} value is expected from the high-resolution photoemission experiments³¹ corroborated with NMR measurements as well.³² Namely, it was suggested that K_{ρ} increases when going from

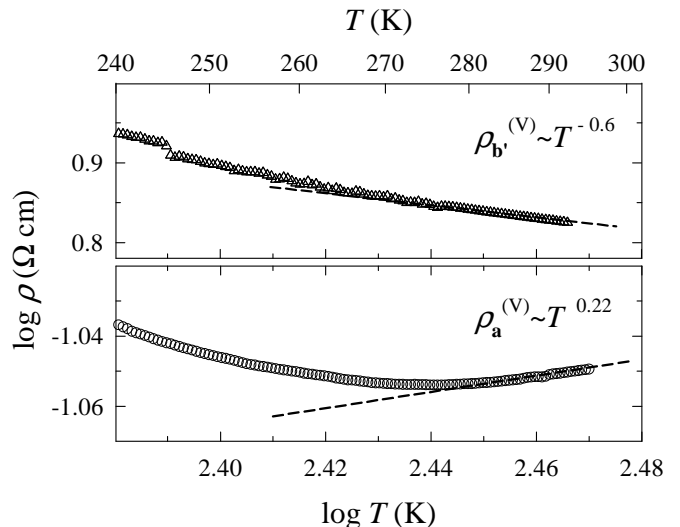


FIG. 5: Temperature dependencies of the constant-volume resistivities $\rho_{\mathbf{a}}^{(V)}$ and $\rho_{\mathbf{b}'}^{(V)}$ (see text for the details of the conversion procedure).

$(\text{TMTTF})_2\text{PF}_6$ to $(\text{TMTSF})_2\text{PF}_6$, leading to a decrease of the $4k_F$ fluctuations and, correlatively, to a decrease of the charge localization temperature. Up to now the measurements of dc transport along the transverse axis performed in $(\text{TMTSF})_2X$ analogs were not fully understood theoretically from the LL picture, since the model was compared with \mathbf{a} and \mathbf{c}^* axis resistivity results. The \mathbf{b}' axis data have shown anomalous exponents and were considered as a crossover between the two regimes.^{23,29} Here, we emphasize that our $(\text{TMTTF})_2\text{AsF}_6$ resistivity results show, for the first time, the agreement with LL model for \mathbf{a} and \mathbf{b} axis. (We are neglecting \mathbf{c} axis because $t_b \gg t_c$.)

Summarizing this part of our results, we point out that the metallic-like behavior is found at high temperature ($T > 240$ K) for $\rho_{\mathbf{a}}$ only, which evidences against a conventional FL picture. Furthermore, the power law of the temperature dependence for the longitudinal and transverse resistivity proposed in the LL model does agree with our $\rho_{\mathbf{a}}^{(V)}(T)$ and $\rho_{\mathbf{b}'}^{(V)}(T)$ experimental results for $T > 260$ K, with $K_{\rho} = 0.20$, favoring the LL description.

Our resistivity results for lower temperatures are consistent with those already published,⁶ showing a broad minimum around $T_{\rho} \approx 240$ K for $\rho_{\mathbf{a}}(T)$ and an increase below T_{ρ} . No change in the magnetic susceptibility (indicating the spin-charge separation) or the change in the structure has been observed at T_{ρ} . It is suggested that the presence of the anomaly of such description indicates that the electronic system is highly correlated. This behavior is a consequence of the continuous opening of a charge gap closely connected to the increased Coulomb interaction and dimerization. However, the results for \mathbf{b}' and \mathbf{c}^* axis do not show any change in slope around T_{ρ} and have not been analyzed up to now. At variance with ordinary semiconductors, only charge degrees of freedom

are thermally activated below T_ρ whereas spin excitations remain gapless, a feature typical of a Mott insulator.⁷

For $T < T_\rho$ the resistivity increases exponentially down to $T_{CO} \approx 100$ K where there is a change of slope (cf. Fig. 1), i.e. a steep increase of the conductivity gap Δ : sharper changes in \mathbf{b}' and \mathbf{c}^* directions indicate an anisotropy of the Δ values. T_{CO} is the temperature where a spontaneous charge disproportionation, or charge ordering, occurs, dividing the molecules into two nonequivalent species as verified using 1D and 2D NMR spectroscopy.⁹ At ambient temperature the spectra are characteristic of nuclei in equivalent molecules. Below a continuous charge-ordering transition temperature T_{CO} , there is evidence for two non-equivalent molecules with unequal electron densities. This is supported by infrared spectroscopy of the EMV-coupled $A_g(\nu_3)$ intramolecular vibration.¹⁰ Below T_{CO} the mode splits in two indicating a charge disproportionation of $\pm 0.13e$. The absence of an associated magnetic anomaly³³ indicates that only the charge degrees of freedom are involved and the lack of evidence for a structural anomaly suggests that charge-lattice coupling is too weak to drive the transition. EXAFS experiments were performed below and above T_{CO} , in order to check a possible displacement of the anion coupled to the charge order.³⁴ No significant difference was observed between the spectra, indicating that the displacement of the anion, if any, is less than 0.05 \AA . The nature of possible phase transition was clarified by discoveries of the huge dielectric anomaly, and the phase transition was interpreted as the one to the ferroelectric (FE) state. It was also suggested that the FE transition is triggered by the uniform shift of ions yielding a macroscopic FE polarization which is gigantically amplified by the charge disproportionation at the molecular stack.³⁵ The fact that the increase in Δ is anisotropic or somehow higher along the \mathbf{b}' and \mathbf{c}^* axes than along the \mathbf{a} axis may further support this suggestion.

B. Hall Effect

The Hall constant R_H of $(\text{TMTTF})_2\text{AsF}_6$ for $T > T_{CO} \approx 100$ K is positive, hole-like and temperature-dependent up to ≈ 200 K. The decrease in $R_H(T)$ with increasing temperature (for $T_{CO} < T < 200$ K) is consistent with the continuous charge localization already pointed out when describing the $\rho_a(T)$ -behavior below T_ρ . Above 200 K, R_H is almost constant with the value around $0.38 \text{ cm}^3\text{C}^{-1}$ (dotted line, Fig. 6).

The confirmation of one-dimensionality and the applicability of LL model at high temperatures ($T > 200$ K) to the transport properties in $(\text{TMTTF})_2\text{AsF}_6$ should be valid for the Hall effect as well. As already mentioned in the introduction, it was concluded from the optical conductivity results for $(\text{TMTCF})_2X$ salts¹⁴ (considered as the strong evidence for LL behavior) that all the dc transport is due to a very low concentration of carriers and that needed to be verified experimentally.

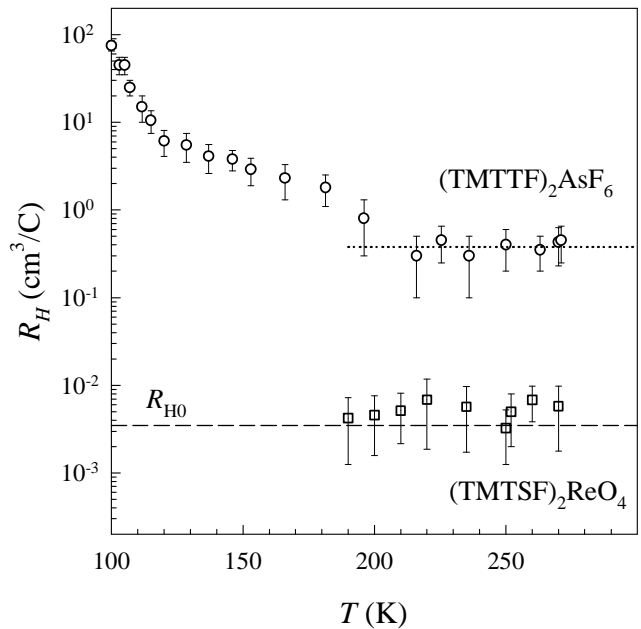


FIG. 6: Temperature dependencies of the Hall coefficient R_H for $(\text{TMTTF})_2\text{AsF}_6$ (circles) and $(\text{TMTSF})_2\text{ReO}_4$ (squares). Above 200 K R_H of $(\text{TMTTF})_2\text{AsF}_6$ has an almost constant value $0.38 \text{ cm}^3\text{C}^{-1}$ (dotted line). The dashed line represents the value $R_{H0} = 3.31 \times 10^{-3} \text{ cm}^3\text{C}^{-1}$ obtained for $(\text{TMTTF})_2\text{AsF}_6$ and the carrier concentration of one hole/unit cell ($n = 1.4 \times 10^{21} \text{ cm}^{-3}$).

Theoretical analysis shows that the Hall coefficient R_H of weakly coupled 1D Luttinger chains does not depend on frequency and temperature, and it is given by a simple formula corresponding to the non-interacting fermions, i.e. $R_H = R_{H0} \approx 1/ne$ (where n is the concentration of carriers). More precisely for quasi-1D systems, using the tight-binding dispersion along the chains, the obtained Hall constant is $R_H = (1/ne)(k_F a / \tan k_F a)$ (where e is the electric charge and $k_F a = \pi/4$).^{36,37} The carrier density for $(\text{TMTCF})_2X$ salts of 1 hole/unit cell gives for $(\text{TMTTF})_2\text{AsF}_6$ $n = 1.48 \times 10^{21} \text{ cm}^{-3}$, and $R_{H0} = 3.31 \times 10^{-3} \text{ cm}^3\text{C}^{-1}$: this is represented as a dashed line in Fig. 6, and this value is about 100 times lower than the experimentally obtained one. In other words, the carrier concentration deduced from the experiment is two orders of magnitude smaller than expected by simple counting arguments, indicating that only a fraction of carriers (about 1%) contribute to the transport. Our findings are in good agreement with the optical investigations as well as with the LL theoretical predictions based on doped Hubbard chains. They strongly evidence the existence of a high temperature regime (above 200 K) in $(\text{TMTTF})_2X$ salts, where 1D physics dominates, i.e. where 1D LL features appear in the transport properties. Here, we would like to repeat that all Hall effect data published up to now were performed for $(\text{TMTSF})_2X$ systems only, and in all those experiments the experimentally obtained R_H values indicated that all the carriers

contribute to the metallic-like transport. Consequently, such data disagreed with the conclusions from the optical conductivity measurements. Moreover, comparing our Hall effect results for $(\text{TMTSF})_2\text{ReO}_4$ (Ref. 18) and $(\text{TMTTF})_2\text{AsF}_6$ (Fig. 6) we find indications that the high temperature transport properties in $(\text{TMTCF})_2X$ salts change their behavior when going from a LL (for $C = \text{S}$) to a FL (for $C = \text{Se}$) regime.

The Hall coefficient exhibits an abrupt change in its temperature dependence around T_{CO} (cf. inset of Fig. 4): R_H changes its sign and its value increases rapidly with the further temperature decrease. While the increase of $R_H(T)$ with the temperature decrease below T_ρ is expected because of a gradual localization of charge carriers, the abrupt change, i.e. the change of sign, around $T_{\text{CO}} \approx 100 \text{ K}$ is surprising since it occurs in the semiconducting state. Note, the change in sign of the Hall coefficient was found at the SDW transition in $(\text{TMTSF})_2\text{PF}_6$ (Refs. 16,17), as well as at the anion ordering transition in $(\text{TMTSF})_2\text{ReO}_4$.¹⁸ In both cases the phase transition is also a metal-insulator transition, connected with the opening of the energy gap and consequently the change in transport mechanism from metallic-like to semiconducting one. On the other hand, the stronger temperature dependence of R_H close to the phase transition followed by the change of sign (indicating that the holes are participating in the electrical transport above and electrons below phase transition) is a common feature in semiconductors.³⁸ As the Hall fields created by electrons and holes are opposing each other, it is apparent that the galvanomagnetic effects can have unusually strong temperature variations in regions where the resultant Hall field is nearly null, when the relative electron-hole population is temperature dependent. Below the CO transition $R_H(T)$ shows the rapid increase with decreasing temperature, i.e. the Hall coefficient is activated as expected for semiconductor. Moreover, the activation energy agrees well with that obtained from the resistivity data. The question arises why the dramatic change in R_H does not occur in the temperature range where the resistivity shows its minimum and the carriers become localized, as identified by the increase of the conductivity gap. Instead, not much change is observed well below T_ρ until charge ordering sets in at the transition T_{CO} . We propose the following interpretation: if one imagines that below T_ρ the gap opens gradually upon cooling, the increase in $R_H(T)$ indicates a decrease in number of carriers (holes) as long as $\Delta(T) \leq k_B T$. In the semiconducting phase around T_{CO} where $\Delta(T) > k_B T$, a transition occurs in which the carriers condense into an insulating charge-ordered state, i.e. our results reflect the exponential freezing out of the carriers below T_{CO} . In line with

these, the abrupt change in $R_H(T)$ around T_{CO} , where an increase of the conductivity gap $\Delta(T)$ occurs, demonstrates a phase transition to a charge ordered state.

V. CONCLUSION

We have found clear evidence that the transport properties of $(\text{TMTTF})_2\text{AsF}_6$ at high temperatures ($T > 200 \text{ K}$) can be understood in terms of the Luttinger-liquid theory which describes 1D systems. This conclusion is based on the metallic-like resistivity along the \mathbf{a} -axis only for $T > T_\rho$, as well as on a good agreement with the power laws predicted for $\rho_{\mathbf{a}}$ (ρ_{\parallel}) and $\rho_{\mathbf{b}'}$ (ρ_{\perp}) from existing LL model. Further support comes from the constant value of the Hall coefficient in the same temperature region, showing a strong reduction in number of carriers participating in dc transport. By comparing the results on $(\text{TMTTF})_2\text{AsF}_6$ with those for $(\text{TMTSF})_2X$ systems (where the LL power laws for the resistivity yield a more complex picture, while R_H has much lower values) we can infer that the high temperature transport properties in $(\text{TMTCF})_2X$ salts change their behavior from a Luttinger liquid to a Fermi liquid when going from $C = \text{S}$ to Se .

At lower temperatures the resistivity data show a semiconducting behavior for all three directions down to $T_{\text{CO}} \approx 100 \text{ K}$, where a charge-ordering transition occurs. This is characterized by a steep increase of the conductivity gap in the resistivity measurements for all three directions, although somehow stronger for the two axes perpendicular to the chains. This may be the consequence of the uniform shift of ions yielding a macroscopic FE polarization as predicted in analysis of dielectric measurements. However, the fact that no significant change in structural measurements was found below T_{CO} weakens this suggestion. On the other hand, the steep increase of the conductivity gap below T_{CO} in resistivity manifests itself as an abrupt change in the $R_H(T)$ behavior: the change of sign and the rapid increasing of its value with further temperature decrease is a strong indication that carriers condense into an insulating charge-ordered state.

Acknowledgments

We thank G. Untereiner for the crystal growth and sample preparation. The work was supported by the Croatian Ministry of Science, Education and Sports, grant 0119251 and 0035015 and the Deutsche Forschungsgemeinschaft (DFG).

* Electronic address: bhamzic@ifs.hr

¹ T. Ishiguro, K. Yamaji, and G. Saito, *Organic superconductors* (Springer, 1998), 2nd ed.

² H. J. Schulz, *Int. J. Mod. Phys. B* **5**, 57 (1991).

³ J. Voit, *Phys. Rev. B* **47**, 6740 (1992).

⁴ T. Giamarchi, *Quantum Physics in One Dimension* (Ox-

- ford University Press, Oxford, 2004).
- ⁵ D. Jérôme, in *Organic Conductors*, edited by J. P. Farges (Marcel Dekker Inc., New York, 1994), p. 405.
 - ⁶ R. Laversanne, C. Coulon, B. Gallois, J. P. Pouget, and R. Moret, *J. Phys. Lett.* **45**, 393 (1984).
 - ⁷ C. Bourbonnais and D. Jérôme, in *Advances in Synthetic Metals, Twenty years of Progress in Science and Technology*, edited by P. Bernier, S. Lefrant, and G. Bidan (Elsevier, New York, 1999), p. 206.
 - ⁸ P. Monceau, F. Y. Nad, and S. Brazovskii, *Phys. Rev. Lett.* **86**, 4080 (2001).
 - ⁹ D. S. Chow, F. Zamborszky, B. Alavi, D. J. Tantillo, A. Baur, C. A. Merlic, and S. E. Brown, *Phys. Rev. Lett.* **85**, 1698 (2000).
 - ¹⁰ M. Dumm, B. Salameh, M. Abaker, L. Montgomery, and M. Dressel, *J. Phys. IV France* **114**, 57 (2004).
 - ¹¹ T. Nakamura, *J. Phys. Soc. Jpn.* **72**, 213 (2003).
 - ¹² B. Salameh, M. Dumm, M. Dressel, and L. Montgomery, unpublished.
 - ¹³ M. Dressel, *Naturwiss.* **90**, 337 (2003).
 - ¹⁴ V. Vescoli, L. Degiorgi, W. Henderson, G. Gruner, K. P. Starkey, and L. K. Montgomery, *Science* **281**, 1155 (1998).
 - ¹⁵ T. Giamarchi, *Physica B: Condensed Matter* **230-232**, 975 (1997).
 - ¹⁶ G. Mihály, I. Kézsmárki, F. Zamborszky, and L. Forró, *Phys. Rev. Lett.* **84**, 2670 (2000).
 - ¹⁷ J. Moser, J. R. Cooper, D. Jérôme, B. Alavi, S. E. Brown, and K. Bechgaard, *Phys. Rev. Lett.* **84**, 2674 (2000).
 - ¹⁸ B. Korin-Hamzić, E. Tafra, M. Basletić, A. Hamzić, G. Untereiner, and M. Dressel, *Phys. Rev. B* **67**, 014513 (2003).
 - ¹⁹ J. R. Cooper and B. Korin-Hamzić, in *Organic Conductors*, edited by J. P. Farges (Marcel Dekker Inc., New York, 1994), p. 359.
 - ²⁰ C. S. Jacobsen, H. J. Pedersen, K. Mortensen, G. Rindorf, N. Thorup, J. B. Torrance, and K. Bechgaard, *Solid State Phys.* **15**, 2657 (1982).
 - ²¹ K. Bechgaard, C. S. Jacobsen, K. Mortensen, J. H. Pedersen, and N. Thorup, *Solid State Commun.* **33**, 1119 (1980).
 - ²² J. R. Cooper, L. Forró, B. Korin-Hamzić, K. Bechgaard, and A. Moradpour, *Phys. Rev. B* **33**, 6810 (1986).
 - ²³ M. Dressel, K. Petukhov, B. Salameh, P. Zornoza, and T. Giamarchi, *Phys. Rev. B* **71**, 075104 (2005).
 - ²⁴ M. Dressel and G. Grüner, in *Electrodynamics of Solids* (Cambridge University Press, Cambridge, 2002).
 - ²⁵ A. Georges, T. Giamarchi, and N. Sandler, *Phys. Rev. B* **61**, 16393 (2000).
 - ²⁶ A. Lopatin, A. Georges, and T. Giamarchi, *Phys. Rev. B* **63**, 075109 (2001).
 - ²⁷ D. Jérôme and H. J. Schulz, *Adv. Phys.* **31**, 299 (1982).
 - ²⁸ P. M. Grant, *J. Phys. (Paris)* **44**, C3 847 (1983).
 - ²⁹ J. Moser, M. Gabay, P. Auban-Senzier, D. Jérôme, K. Bechgaard, and J. M. Fabre, *Europhys. J. B* **1**, 39 (1998).
 - ³⁰ A. T. Zheleznyak and V. M. Yakovenko, *Europhys. J. B* **11**, 385 (1999).
 - ³¹ B. Dardel, D. Malterre, M. Grioni, P. Weibel, Y. Baer, J. Voit, and D. Jérôme, *Europhys. Lett.* **24**, 687 (1993).
 - ³² P. Wzietek, F. Creuzet, D. Jérôme, K. Bechgaard, and P. Batail, *J. Phys. I* **3**, 171 (1993).
 - ³³ Except for some increase of the ESR linewidth below T_{CO} due to changes in the relaxation process. See Refs. 11,12.
 - ³⁴ S. Ravy, P. Foury-Leylekian, D. L. Bolloc'h, J. P. Pouget, J. M. Fabre, R. J. Prado, and P. Lagarde, *J. Phys. IV France* **114**, 81 (2004).
 - ³⁵ S. Brazovskii, *J. Phys. IV France* **114**, 9 (2004).
 - ³⁶ J. R. Cooper, M. Miljak, G. Delpanque, D. Jérôme, M. Wager, J. M. Fabre, and L. Giral, *J. Phys. (Paris)* **38**, 1097 (1977).
 - ³⁷ K. Maki and A. Virosztek, *Phys. Rev. B* **41**, 557 (1990).
 - ³⁸ A. C. Beer, *Galvanomagnetic Effects in Semiconductors* (Academic Press, London, 1963).